INTERNATIONAL JOURNAL FOR NUMERICAL METHODS IN FLUIDS, VOL. 14, 83–93 (1992)

HEAT TRANSFER DURING MELTING IN RECTANGULAR ENCLOSURES—A FINITE ELEMENT ANALYSIS

A. SARKAR AND V. M. K. SASTRI

Department of Mechanical Engineering, Indian Institute of Technology, Madras 600 036, India

SUMMARY

This paper is devoted to the finite element analysis of heat transfer during melting in rectangular enclosures. The effects of aspect ratio and subcooling on the motion of the interface and the Nusselt number have been investigated. The different schemes employed in the present work throw useful light on the choice of the appropriate method for dealing with such phase change problems.

KEY WORDS Phase change material (PCM) Finite element analysis Enclosures

INTRODUCTION

Over the last few years a considerable amount of experimental and numerical research has been carried out to determine the role of natural convection in the kinetics of heat transfer during the melting of a solid phase change material (PCM). Typical application areas of current interest include thermal energy storage devices, casting technology and nuclear power, especially in the area of accident analysis.[1] The results have been presented for several different geometries, the approach being essentially two-dimensional. The configurations most widely studied are the horizontal cylinder, the vertical cylinder and the rectangular enclosure.

Most of the experiments employed *n*-octadecane as the PCM, although Gau and Viskanta[2] also reported results for gallium. Van Buren and Viskanta[3] carried out an interferometric study on *n*-octadecane and concluded that such studies should be restricted to natural convection phenomena with small temperature differences because of the difficulty in interpreting the high fringe density produced by larger temperature differences. Webb and Viskanta[4] studied the melting heat transfer in an inclined rectangular enclosure. In typical thermal storage applications the Rayleigh number in the liquid region is very high, typically in the range from 10^6 to 10^9.[5]

Experiments[6] indicate that the flow remains entirely laminar in this range of Rayleigh numbers, the transition to turbulence occurring only beyond Rayleigh numbers of 10^{10}. Such high-Rayleigh-number flow is characterized by fast-moving thin shear layers through which most of the heat transfer takes place, while the region away from the walls, often called the 'core region', is mostly inactive.[5] Most numerical studies conducted so far have employed efficient finite difference schemes to solve the steady state convection problem, using a false transient procedure to accelerate convergence. Bearing in mind the difficulty of treating the conservation equations in a non-orthogonal cavity, some authors have used the method of transformation. Gobin and co-workers[5,7,8] used a linear transformation technique for transforming a non-orthogonal cavity into an orthogonal one. The resulting conservation equations are simplified by neglecting the

0271–2091/92/010083–11$05.50

Received February 1990
Revised January 1991

cross terms due to the non-orthogonality of the co-ordinate transformation. Ho and Viskanta,[9] however, used a streamfunction–vorticity function formulation in which the cross-differential terms have been considered and these cross terms have been evaluated from the values of the variables at the previous time step. The prospects of the fixed grid method have also been explored in considerable detail. The main problem with fixed grids is in accounting for the zero-velocity condition as the liquid region turns to solid. Morgan[10] employs the simple approach of fixing the velocities to zero in a computational cell whenever the mean latent heat content ΔH reaches some predetermined value between zero and L, where L is the latent heat of phase change. Gartling[1] employed a similar approach by assuming the viscosity to be a function of ΔH such that as ΔH decreases from L to zero, the viscosity increases to a large value. Voller *et al.*[11–13,20] investigated various ways of dealing with zero solid velocities in fixed grid enthalpy solutions of freezing in a thermal cavity formulation for the numerical solution of convection–diffusion-controlled mushy region phase change problems. The potential of the finite element method has revived interest in the past few years in the solution of phase change problems. The objective of the present work is to investigate the conventional problem of melting of a pure phase change material from an isothermal vertical surface by employing the finite element method. The effect of various degrees of subcooling has also been reported.

FORMULATION OF THE PROBLEM

Consider the two-dimensional melting of a solid PCM from an isothermal vertical wall (Figure 1). The solid PCM may be initially at the fusion temperature T_m or may be maintained at a temperature below T_m. The bottom and top free surfaces are assumed to be insulated. Accordingly, the problem be treated as a one-region or two-region one. The following further assumptions are made.

1. The thermophysical properties of the material undergoing phase change are constant.
2. The density variation in the liquid is considered only insofar as it contributes to buoyancy, but is otherwise neglected, i.e. the Boussinesq approximation is valid.
3. The liquid is assumed to be Newtonian.
4. Two-dimensional laminar flow is considered.
5. The heat transfer near the topmost portion of the melt, due to the expansion of the PCM upon melting, has been neglected.
6. The melt front surface is smooth, i.e. there are no effects arising from dendrite formation or coarse-grained crystal structure in the solid.
7. The whole melting process may be considered to consist of a number of quasi-static processes.
8. The effect of surface tension along the free surface is also neglected.

As far as the assumption of a quasistatic process is concerned, it is worthwhile to mention the following experimental observation:[14] the velocity of propagation of the melt front was of the order of $3 \times 10^{-6}\,\mathrm{m\,s^{-1}}$, which was several orders of magnitude smaller than the fluid velocities, which were of the order of $3 \times 10^{-3}\,\mathrm{m\,s^{-1}}$, in the boundary layers on the vertical walls. This suggests that the calculation of the melt front motion can be decoupled from the calculation of the natural convection flow in the melt region by dividing the process into a number of quasi-static processes. Thus for a given melt cavity the conservation equations are solved first, then the heat fluxes along the interface are calculated. In the case of subcooling, the solid side heat fluxes have also to be calculated. The final position of the interface is then obtained by solving the interface energy equation. As soon as the melt cavity is defined, the steps are repeated. Regarding the

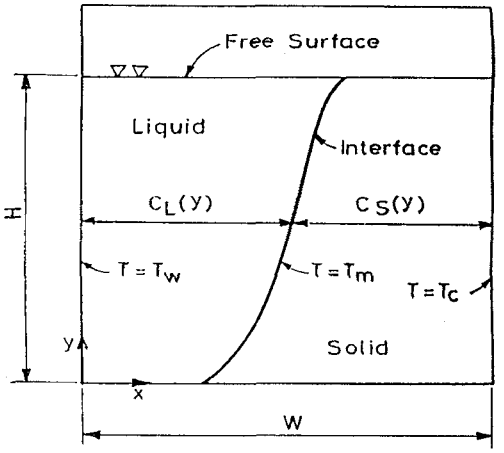

Figure 1. The problem under consideration

choice of the value of the Stefan number, it is worthwhile to mention that for Stefan numbers greater than 0·2 the quasi-static assumption may not be valid since the fluid flow velocity and the melt front velocity may be comparable. However, the aforesaid limit on the Stefan number can be driven up if there is a considerable amount of subcooling since subcooling is known to impede the melting process.

The conservation equations, after non-dimensionalization, may be written as

$$\partial U/\partial X + \partial V/\partial Y = 0, \tag{1a}$$

$$U\partial U/\partial X + V\partial U/\partial Y = -\partial P/\partial X + (\partial^2 U/\partial X^2 + \partial^2 U/\partial Y^2)/A, \tag{1b}$$

$$U\partial V/\partial X + V\partial V/\partial Y = -\partial P/\partial Y + (\partial^2 V/\partial X^2 + \partial^2 V/\partial Y^2)/A + \theta, \tag{1c}$$

$$U\partial\theta/\partial X + V\partial\theta/\partial Y = (\partial^2\theta/\partial Y + \partial^2\theta/\partial Y^2)/APr. \tag{1d}$$

The following non-dimensional quantities have been introduced:

$$U = u/u_0, \qquad V = v/u_0, \qquad P = p/\rho u_0^2, \qquad X = x/H,$$

$$Y = y/H, \qquad \theta = (T - T_m)/(T_w - T_m), \qquad A = (Ra_H/Pr)^{1/2}.$$

The boundary conditions are as follows:

(a) at $X = 0$: $U = V = 0$, $\theta = 1$;

(b) at $Y = 0$: $U = V = 0$, $\partial\theta/\partial Y = 0$;

(c) at $Y = 1$: $V = 0$, $\partial\theta/\partial Y = 0$, $\partial U/\partial Y = 0$.

The additional boundary conditon in (c) for the free surface, i.e. $\partial U/\partial Y = 0$, does not necessitate any special attention in the finite element method since it is taken care of by the inter-element continuity requirement.

(d) at $X = W/H$: $U = V = 0$, $\theta = -SC/Ste$;

at the interface: $U = V = 0$, $\theta = 0$.

In the case of subcooling, i.e. the case for which $T_c < T_m$, the conduction in the solid phase must be considered. Finally, the non-dimensional energy equation at the interface is given by

$$\partial \bar{S}/\partial(Fo) = Ste(\nabla\theta_S \cdot \mathbf{n} - \nabla\theta_L \cdot \mathbf{n}),$$

where $\mathbf{n}$ is the local normal to the interface.

Melting of a pure substance in a rectangular enclosure is characterized by five dimensionless parameters: Rayleigh number (based on height), Prandtl number, Stefan number, aspect ratio and subcooling parameter.

Discretization of the aforesaid equations has been carried out by Galerkin's method. The basic element used for the computations is an eight-noded isoparametric quadrilateral in which quadratic 'serendipity' functions are used to approximate the velocity and temperature. However, linear interpolating functions are used for the pressure.[15] Details of the formulation and method of solution are discussed in Reference 16. For the sake of brevity it is noted that the non-linearities in the discretized equations are treated by a Newton–Raphson method and the resulting simultaneous equations are solved by a frontal solver.[17] During the iteration process the largest value of the residue at each iteration was noted. The process was assumed to have converged when the largest residue reached preassigned value as low as 0·00005. At convergence the absolute value of the difference between two successively iterated values of any variable did not exceed 0·0001.

Initially we attempted to solve the phase change problem in the absence of subcooling. The space discretization was confined to the liquid zone only since the problem was essentially a one-region problem. Initial results were promising. The major advantage of this was that nodes could be placed along the interface boundary and no-slip boundary conditions could be easily incorporated. However, as the curvature of the interface increased, we experienced difficulty in getting an accurate solution. We then concentrated on the fixed grid method as outlined by Gartling.[1] In this method the whole area occuped by the PCM was discretized once and for all to obviate the basic source of error associated with the earlier method, i.e. too much deformation of the eight-noded isoparametric quadrilateral element may prevent satisfactory functioning of the transformation functions. Then in the fixed grid method the interface was allowed to traverse the computational domain. The most important aspect of this method was that the same conservation equations were used for both phases, including the elements that contain a mixture of liquid and solid PCM. The distinction between the solid and liquid phases was made by declaring the viscosity to be space-dependent and a 'high' value of the viscosity was assigned to the element nodes that fell in the solid phase. According to our experience, too 'high' a value of the viscosity may result in an ill-conditioned matrix. Moreover, since a finite value of 'high' viscosity was used, it may be inferred that at best a solid phase is being 'approached' from the computational viewpoint.

The next difficulty was to assign the no-slip conditions at the interface. Since in the fixed grid method the interface need not coincide with the nodes, a zeroth-order solution can be envisaged by assigning no-slip conditions at the nodes nearest to the predetermined interface position. Although the method looks straightforward from the computational point of view, we experienced difficulties in confining the flow to the liquid zone alone and significantly 'high' values of the velocities were observed at nodes in the 'solid' phase.

At this stage we had to abandon the work on the fixed grid method. However, the results were better compared to the earlier method and we feel that with the introduction of higher-order elements with larger number of nodes the method may yield satisfactory results. A detailed discussion on the application of the fixed grid method can be found in Reference 18.

PRESENT METHOD

Consider the PCM (Figure 1) at its fusion temperature, i.e. there is no subcooling. An attempt is made to transform the irregular-shaped liquid cavity into an orthogonal computational space by using the transformation

$$\bar{Y}=Y, \qquad \bar{X}=X/C_{\mathrm{L}}(Y). \tag{2}$$

This results in a square-shaped computational domain. However, with the introduction of this transformation the conservation equation (1a)–(1d) take the form

continuity: $$\bar{\nabla}\mathbf{V}=0; \tag{3a}$$

momentum: $$(\mathbf{V}\cdot\bar{\nabla})\mathbf{V}=-\bar{\nabla}P+\theta\mathbf{z}+(\bar{\nabla}^2\mathbf{V})/A; \tag{3b}$$

energy: $$(\mathbf{V}\cdot\bar{\nabla})\theta=\bar{\nabla}^2\theta/APr. \tag{3c}$$

Here $\mathbf{z}$ is the unit vector in the direction of gravity and

$$\bar{\nabla}=\frac{1}{C_{\mathrm{L}}}\frac{\partial}{\partial\bar{x}}\mathbf{i}+\frac{\partial}{\partial\bar{y}}\mathbf{j}, \qquad \bar{\nabla}^2=\frac{1}{C_{\mathrm{L}}^2}\frac{\partial^2}{\partial\bar{x}^2}+\frac{\partial^2}{\partial\bar{y}^2}.$$

The corresponding boundary conditions in the computational domain become

(a) at $\bar{X}=0$: $U=V=0$, $\theta=1$;

(b) at $\bar{X}=1$: $U=V=0$, $\theta=0$;

(c) at $\bar{Y}=0$: $U=V=0$, $\partial\theta/\partial\bar{Y}=0$;

(d) at $\bar{Y}=1$: $V=0$, $\partial\theta/\partial\bar{Y}=0$.

The transformation function $C_{\mathrm{L}}(Y)$ is usually called the melt front shape function or stretching function and is required to be defined not only for the nodes along the interface but also for other nodes in the liquid zone. In the case of subcooling, another shape function $C_{\mathrm{S}}(Y)$ (Figure 1) can be defined and a similar transformation will result in another square computational domain in which the following relation holds: $C_{\mathrm{L}}(Y)+C_{\mathrm{S}}(Y)=W/H$. The conduction equation is then solved in this computational plane with two different side wall temperatures as discussed earlier, while the two horizontal surfaces are assumed to be insulated.

The numerical simulation is initiated by assuming the existence of a thin melt layer in which the classical Stefan solution is valid. This melt volume corresponds to less than 6% of the total melt. It is also assumed that the shape of this initial melt does not significantly affect the subsequent evolution of the melt front. At each quasi-static step the governing equations (3a)–(3c) are solved in the orthogonal computational domain with the associated boundary conditions. Upon convergence, the criterion of which has been discussed earlier, the temperature and flow fields are referred back to the physical domain. Heat fluxes are calculated and interface displacements are obtained by employing the interface energy balance equation. A cubic spline is then fitted through these points to obtain a smooth interface shape. The new domain is again discretized and the melt front shape functions, i.e. C_{L}, are determined at the interface nodes. Shape functions at the interior nodes are calculated using linear interpolation. The process is then repeated. In the computational domain the x- and y-extends in the region around the cold corners, particularly the one near the interface, are not allowed to exceed 0·01. The non-dimensional time step is taken as 0·00001 for each quasi-static step. Consequently, a large number of simulation. steps have to be performed to obtain a significant amount of melt. It has also been observed that the number of

iterations required to attain convergence for a quasi-static step may be as low as three during the initial period of melting and may even run up to eight with the full onset of convection. On average it takes around 400 CPU time on a Siemens 7580E system for each quasi-static step.

RESULTS AND DISCUSSION

The results for the cases of zero nd non-zero subcooling are obtained for $Ra = 10^8$, $Pr = 50$ and $Ste = 0{\cdot}2$.

Zero subcooling

Figure 2 shows the evolution of the melt front profiles for two different aspect ratios, i.e. 5·25 and 2·44, for zero subcooling. In the interest of clarity, only one melt front shape in each case has been compared with experiment.[19] It is interesting to note that the interface in effect represents a zero isotherm. During the initial period, heat transfer is dominated by conduction, a fact which is confirmed by the presence of an almost vertical zero isotherm, i.e. the interface. As heating is continued, the upper part of the interface near the free surface becomes slightly curved. This earlier departure of the melting behaviour from the conduction-dominated regime may be attributed to the presence of density-induced melt motion resulting from the volume increase

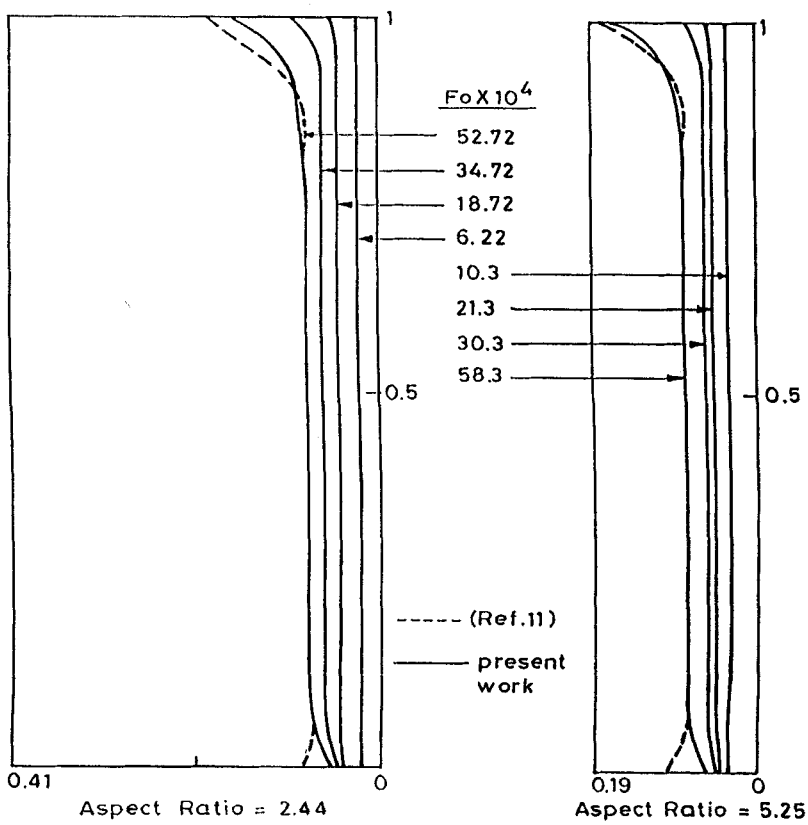

Figure 2. Time evolution of melt front profiles (cold wall on left)

which accompanies the phase change. Another interesting possibility is the existence of surface tension along the free surface. During the initial period of melting, the melt cavity being very shallow, surface tension may have a significant role in the heat transfer, at least around the region near the interface. As heating is continued still further, the mode of heat transfer gradually changes from conduction to natural convection. Liquid melt around the hot wall, while moving up, receives heat from the wall and attains its maximum temperature near the free surface. It then takes a 90° turn and flows towards the cold interface where maximum heat transfer occurs. During its journey downwards, it continues transferring heat to the interface and its temperature decreases. Hence it is easy to perceive that maximum melting will occur at the top while the least amount of melting is expected at the bottom. Figure 3 demonstrates the pattern of streamlines with fully developed natural convection conditions in a melt cavity with an aspect ratio of 5·25 and zero subcooling. It clearly shows the presence of a strong recirculating flow within the melt cavity. The disagreement at the bottom of the interface is attributed to the fact that a considerable amount of conduction occurs along the bottom plate of the container in the experiment.[19]

Figure 4 shows the considerable influence of the aspect ratio on the melt fraction. This result is of considerable practical interest since it has a bearing on optimizing the dimensions of latent heat storage elements. Gadgil and Gobin[5] presented the same type of results, but the flow parameter, i.e. Ra_H, was not held constant. Hence the effect of the aspect ratio on the melt fraction is closely associated with Ra_H in their work. To make the comparison more effective, the flow parameters

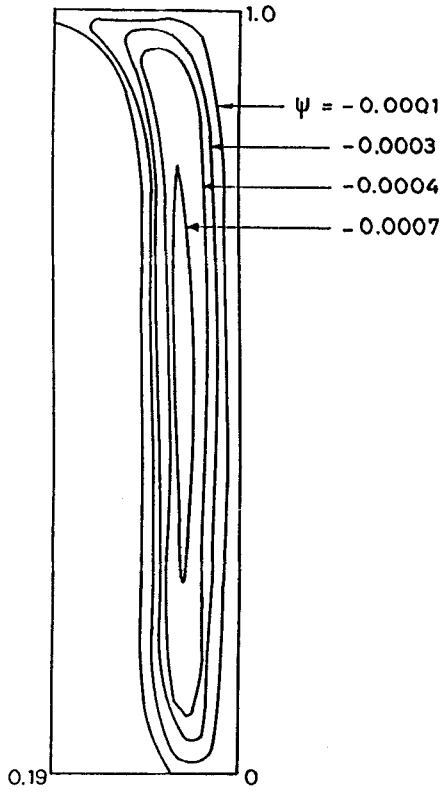

Figure 3. Streamlines at $Fo = 78 \times 10^{-4}$ for aspect ratio of 5·25 and $SC = 0$

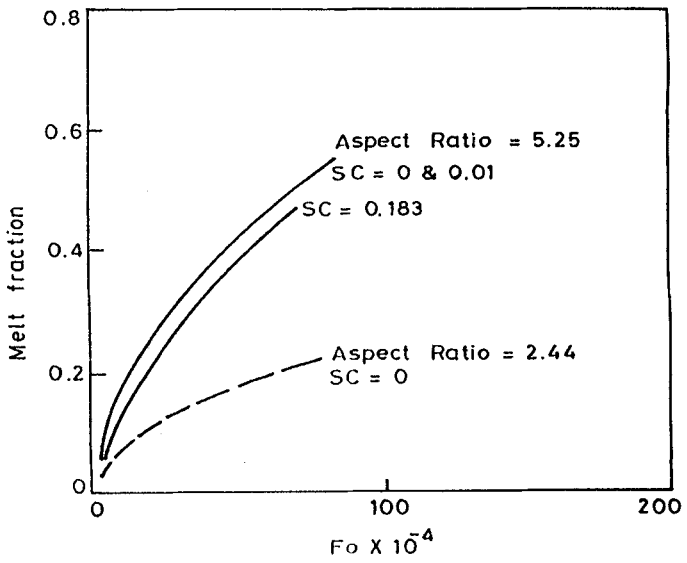

Figure 4. Melt fraction versus time

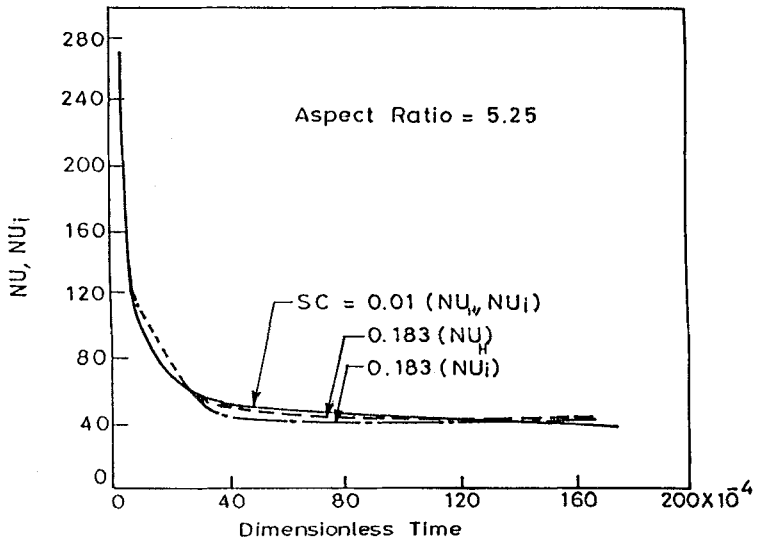

Figure 5. Nusselt number versus time

have been held constant in the present work. The diverging nature of the melt fraction curves clearly indicates that the higher the aspect ratio, the higher is the melt fraction.

Figure 5 exhibits the variation of Nusselt number with dimensionless time. It shows that the Nusselt number starts with a value of the order of 250. As the cavity widens, Nu_H rapidly decreases until the cavity is wide enough to allow the onset of fully developed convection.

This slows down the decrease in Nusselt number. It may also be observed that with elapse of time the trend of the Nusselt number assumes an asymptotic nature, a phenomenon which is

explained by the fact that when the cavity is wide enough, any subsequent event around the interface does not significantly alter the thermal field around the hot wall.

Non-zero subcooling

Two cases with different subcooling parameters have been considered. Figure 6 shows the time evolution of the melt front profiles for subcooling parameters of 0·01 and 0·183. Figure 4 shows the variation of melt fraction with dimensionless time. It may be observed that although the initial melt fraction has been kept the same, the melt fraction curves diverge slowly. At any given time the melt fraction is greater with lower subcooling, indicating that subcooling impedes the development of the melt front.

Figure 5 shows the Nusselt numbers at the hot wall and the interface (Nu_i) as functions of dimensionless time. The difference between the two Nusselt numbers under subcooling conditions is observed to be small. This is due to the fact that the temperature field is not affected significantly by subcooling. Within the limits of the melt fraction in the present study, it has been observed that subcooling tends to assert a larger and larger influence on the interface Nusselt number as the melt front approaches the other end of the container. It is somewhat evident from Figure 5 that the two Nusselt numbers diverge very slowly for a subcooling parameter of 0·183,

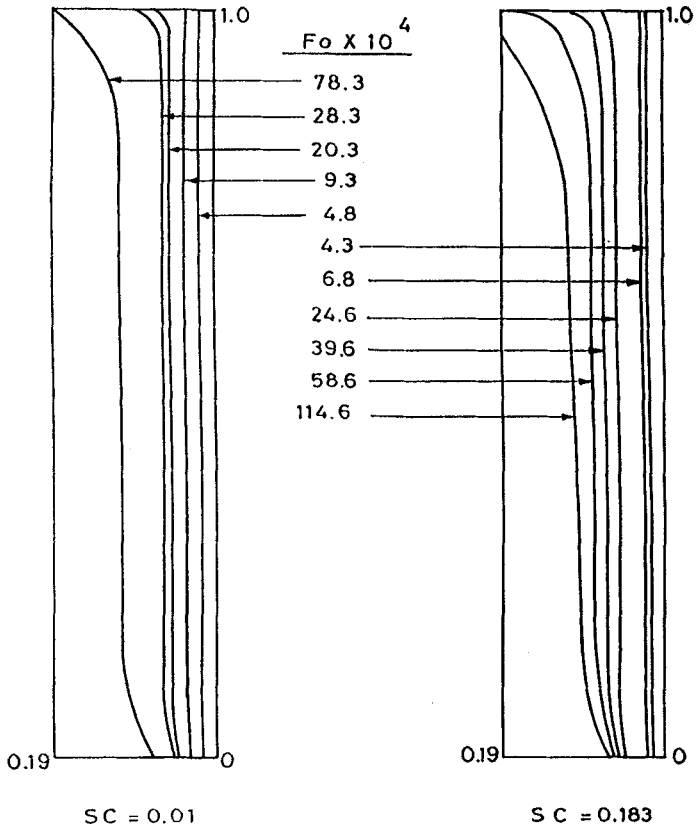

Figure 6. Time evolution of melt front profile for aspect ratio of 5·25 (cold wall on left)

while for $SC = 0{\cdot}01$ the two curves almost coincide. This coincidence is expected to be lost near the end. In the light of these observations we attempted to compute the hot wall Nusselt number when the PCM has melted completely. The result was that a very high value of Nu_H was obtained. For example, the value of Nu_H was 75 while the asymptotic behaviour of Nu_H for $SC = 0{\cdot}183$ indicates that Nu_H should be around 40 (Figure 5). This anomaly is explained by the fact that for 100% melt the temperature differential is between unity at the hot wall and $-0{\cdot}915$ at the cold wall, while in other cases, when some solid PCM still exists, the driving potential in the liquid melt is between unity and zero. Then, for the 100% melt condition, there is a sudden increase in driving potential across the liquid melt. This observation indicates that any extrapolation towards obtaining Nu_H for 100% melt should not be attempted when the value of the subcooling parameter is high. Hence a relatively close agreement is expected for $SC = 0{\cdot}01$. In fact, for $SC = 0{\cdot}01$ the computed value of Nu_H for 100% melt is found to be 36, while the trend as evident from Figure 5 shows that the expected value will be around 38.

CONCLUSIONS

The performance of the present method of employing the transformation seems to work quite well. However, it is worthwhile to mention that the transformation works very well as long as $\partial C_L/\partial y \leqslant 0{\cdot}3$.[7] Hence near the top, where the interface is very much curved, some discrepancies are expected to occur. This is probably due to the neglect of first- and higher-order derivatives of C_L while transforming the natural conservation equations.

APPENDIX: NOMENCLATURE

x, y	dimensional co-ordinates
X, Y	physical dimensionless co-ordinates in transformed computational domain
H	wetted height of enclosure
W	width of enclosure
u, v	horizontal and vertical components of velocity
U, V	non-dimensional velocities
P	non-dimensional pressure
p	pressure
Pr	Prandtl number, ν/α
Ra_H	Rayleigh number (based on H), $Gr_H\, Pr$
Gr_H	Grashof number, $\beta g(T_w - T_m)H^3/\nu^2$
g	acceleration due to gravity
T_w, T_c	temperature of hot and cold walls
T_m	melting point of PCM
Ste	Stefan number, $C_p(T_w - T_m)/L$
L	latent heat of fusion
SC	subcooling parameter, $C_p(T_m - T_c)/L$
Fo	non-dimensional time, $\alpha\tau/H^2$
Nu_H	Nusselt number at hot wall (average), $\int_0^1 (\nabla\theta \cdot \mathbf{n})_{X=0}\, dY$
Γ	non-dimensional length of interface
Nu_i	average Nusselt number at interface based on difference between liquid and solid side heat fluxes, $\int_\Gamma [(\nabla\theta \cdot \mathbf{n})_L - (\nabla\theta \cdot \mathbf{n})_S]\, dr / \int_\Gamma dr$
$\bar{S}$	non-dimensional displacement of interface

Greek symbols

α	thermal diffusivity of liquid PCM
β	expansion coefficient
ν	viscosity of liquid PCM
θ	dimensionless temperature, $(T-T_m)/T_w T_m$
τ	dimensional time

REFERENCES

1. D. K. Gartling, 'Finite element analysis of convective heat transfer problems with change of phase', in *Computer Methods in Fluids*, Pentech, London, 1980, pp. 257–284.
2. C. Gau and R. Viskanta, 'Effect of crystal Anisotropy on heat transfer during melting and solidification of a metal', *J. Heat Transfer, Trans. ASME*, **107**, 706–708 (1985).
3. P. D. Van Buren and R. Viskanta, 'Interferometric measurement of heat transfer during melting from a vertical surface', *Int. J. Heat Mass Transfer*, **23**, 568–571 (1980).
4. B. W. Webb and R. Viskanta, 'Natural convection dominated melting heat transfer in an inclined rectangular enclosure', *Int. J. Heat Mass Transfer*, **29**(2), 183–192 (1986).
5. A. Gadgil and D. Gobin, 'Analysis of two dimensional melting in rectangular enclosures in presence of convection', *J. Heat Transfer, Trans. ASME*, **106**, 20–26 (1984).
6. M. W. Nansteel and R. Grief, 'Natural convection heat transfer in undivided and partially divided rectangular enclosures', *J. Heat Transfer, Trans. ASME*, **103**, 623–629 (1981).
7. C. Benard, D. Gobin and F. Martinez, 'Melting in rectangular enclosures: experiments and numerical simulation', *J. Heat Transfer, Trans. ASME*, **107**, 794–803 (1985).
8. C. Benard, D. Gobin and A. Zanali, 'Moving boundary problem: heat conduction in the solid phase of a phase-change material during melting driven by natural convection in the liquid', *Int. J. Heat Mass Transfer*, **29**, 1669–1681 (1986).
9. C.-J. Ho and R. Viskanta, 'Heat transfer during melting from an isothermal vertical wall', *J. Heat Transfer, Trans. ASME*, **106**, 12–19 (1984).
10. K. Morgan, 'A numerical analysis of freezing and melting with convection', *Comput. Methods Appl. Mech. Eng.*, **28**, 275–284 (1981).
11. V. R. Voller, N. C. Markatos and M. Cross, 'Techniques for accounting for the moving interface in convection/diffusion phase change', in R. W. Lewis and K. Morgan (eds.), *Numerical Methods in Thermal Problems Vol. 4*, Pineridge, Swansea, 1985, pp. 595–609.
12. V. R. Voller, N. C. Markatos and M. Cross, 'Solidification in convection and diffusion', in N. C. Markatos *et al.*, (eds), *Numerical Simulations of Fluid Flow and Heat/Mass Transfer Processes*, Springer, Berlin, 1986, pp. 425–432.
13. V. R. Voller, M. Cross and N. C. Markatos, 'An enthalpy method for convection/diffusion phase changes', *Int. j. numer. methods eng.*, **24**, 271–284 (1987).
14. A. Sanson Ortega, C. Benard and D. Gobin, 'Paraffin Trombe wall for space heating', *Proc. Int. Conf. on Building Energy Management*, Porto, 1980.
15. M. D. Olson and S. Y. Tuann, 'Primitive variables versus stream function finite element solutions of Navier Stokes equations', *Finite Elements in Fluids*, **3**, 73–87 (1978).
16. A. Sarkar and V. M. K. Sastri, 'Finite element solution of steady, two dimensional natural convection equations', *Proc. Sixth. Int. Conf. on Numerical Methods in Thermal Problems*, Swansea, 1989, Vol. 2, pp. 1732–1742.
17. P. Hood, 'Frontal solution program for unsymmetric matrices', *Int. j. numer. methods eng.*, **10**, 379–399 (1976).
18. A. Sarkar and V. M. K. Sastri, 'Finite element analysis of two dimensional melting in rectangular enclosures in the presence of convection', *Proc. 9th Int. Heat Transfer Conf.*, Jerusalem, 1990, Hemisphere Publishing Corporation, Vol. 4, pp. 241–246.
19. N. W. Hale and R. Viskanta, 'Photographic observations of the liquid–solid interface motion during melting of a solid heated from an isothermal vertical wall', *Lett. Heat Mass Transfer*, **5**, 329 (1978).
20. V. R. Voller and C. Prakash, 'A fixed grid numerical modelling methodology for convection diffusion mushy region phase change problems', *Int. J. Heat Mass Transfer*, **30**, 1709–1719 (1987).